Waste Management & Research

http://wmr.sagepub.com/

Numerical study of co-firing pulverized coal and biomass inside a cement calciner

Hrvoje Mikulcic, Eberhard von Berg, Milan Vujanovic and Neven Duic

Waste Manag Res 2014 32: 661 originally published online 24 June 2014
DOI: 10.1177/0734242X14538309

The online version of this article can be found at:
http://wmr.sagepub.com/content/32/7/661

Published by:

http://www.sagepublications.com

On behalf of:

International Solid Waste Association

Additional services and information for *Waste Management & Research* can be found at:

Email Alerts: http://wmr.sagepub.com/cgi/alerts

Subscriptions: http://wmr.sagepub.com/subscriptions

Reprints: http://www.sagepub.com/journalsReprints.nav

Permissions: http://www.sagepub.com/journalsPermissions.nav

Citations: http://wmr.sagepub.com/content/32/7/661.refs.html

>> Version of Record - Jul 10, 2014

OnlineFirst Version of Record - Jun 24, 2014

What is This?

Downloaded from wmr.sagepub.com by guest on July 10, 2014

Original Article

WM&R

Waste Management & Research
2014, Vol. 32(7) 661–669
© The Author(s) 2014
Reprints and permissions:
sagepub.co.uk/journalsPermissions.nav
DOI: 10.1177/0734242X14538309
wmr.sagepub.com
SAGE

Numerical study of co-firing pulverized coal and biomass inside a cement calciner

Hrvoje Mikulčić[1], Eberhard von Berg[2], Milan Vujanović[1] and Neven Duić[1]

Abstract

The use of waste wood biomass as fuel is increasingly gaining significance in the cement industry. The combustion of biomass and particularly co-firing of biomass and coal in existing pulverized-fuel burners still faces significant challenges. One possibility for the *ex ante* control and investigation of the co-firing process are computational fluid dynamics (CFD) simulations. The purpose of this paper is to present a numerical analysis of co-firing pulverized coal and biomass in a cement calciner. Numerical models of pulverized coal and biomass combustion were developed and implemented into a commercial CFD code FIRE, which was then used for the analysis. Three-dimensional geometry of a real industrial cement calciner was used for the analysis. Three different co-firing cases were analysed. The results obtained from this study can be used for assessing different co-firing cases, and for improving the understanding of the co-firing process inside the calculated calciner.

Keywords

Cement calciner, co-firing, coal, biomass, calcination process, CFD

Introduction

Over recent decades, the utilization of biomass for energy generation is constantly gaining more and more on importance (Sommer and Ragossnig, 2011). It is already an important mode of fuel utilization in the electric and heat power generation industry and in some process industries. The annual usage of biomass currently represents approximately 8–14% of the world final energy consumption (Ćosić et al., 2011; Williams et al., 2012). This is a result of increased environmental awareness, the effect of global warming and particularly because biomass is a unique renewable resource that directly replaces the use of fossil fuels (Vad Mathiesen et al., 2012). The cement industry is one of the largest carbon-emitting industrial sectors in the EU and in the world, accounting for approximately 4.1% of EU, and around 5% of world anthropogenic CO_2 emissions (Mikulčić et al., 2013a). In line with the EU commitment to combat climate change, the cement industry, as the third largest carbon-emitting industrial sector, needs to reduce its carbon emission significantly. Due to the need for lowering CO_2 emissions, biomass fuels are to some extent already replacing fossil fuels (Fodor and Klemeš, 2012). Unlike fossil fuels, biomass fuels are considered CO_2 neutral, and can be considered renewable, in the sense that the CO_2 generated by biomass combustion recycles from the atmosphere to the plants that replace the fuel, e.g. to the waste wood or energy crops. Since biomass, including biomass residue, decays and produces methane and other decomposition products that greatly exceed the potency of CO_2 as greenhouse gas, the use of biomass as fuel actually has the potential to decrease greenhouse gas impacts, and not just being neutral (Lu et al., 2008; Ragossnig et al., 2009). Combustion of biomass and especially co-combustion of biomass and coal are modes of fuel utilization that are increasingly gaining in significance in the cement industry (Schneider and Ragossnig, 2013; Thomanetz, 2012).

The development of appropriate combustion units is often very demanding, and time and cost consuming. One possibility for the control and investigation of the biomass combustion and co-combustion process involves computational fluid dynamics (CFD) simulations (Klemeš et al., 2010). Early comprehensive information, parametric studies and initial conclusions that can be gained from CFD simulations are very important in handling modern combustion units. Together with experiments and theory, CFD has become an integral component of combustion research. It has been used in the development process for understanding the complex phenomena occurring within the combustion units. However, CFD simulations of biomass combustion and co-combustion still face significant challenges.

[1]Faculty of Mechanical Engineering and Naval Architecture, University of Zagreb, Zagreb, Croatia
[2]AVL–AST, Hans List Platz 1, Graz, Austria

Corresponding author:
Hrvoje Mikulčić, Faculty of Mechanical Engineering and Naval Architecture, University of Zagreb, Ivana Lucica 5, 10000 Zagreb, Croatia.
Email: hrvoje.mikulcic@fsb.hr

Downloaded from wmr.sagepub.com by guest on July 10, 2014

There have been numerous studies that have investigated the biomass combustion on a single-particle level and in real industrial furnaces. Yang et al. (2008) investigated the combustion effects of a single biomass particle. That study showed that the isothermal particle assumption is no longer valid when the particle size exceeds 150–200 μm. This has profound implications on CFD modelling of biomass particles in pulverized fuel furnaces. Momeni et al. (2013) studied the ignition and combustion of biomass particles. That study showed that higher oxygen concentration and higher oxidizer temperature can greatly accelerate the ignition, devolatilization process and char combustion. Ma et al. (2007) using an Eulerian–Lagrangian frame of reference, numerically investigating the combustion of pulverized biomass in a 1-MW industrial test furnace. The numerical predictions obtained by that study showed good agreement with the measured data. However, the use of CFD for investigating the use of biomass as a fuel in cement pyroprocessing units has until now not been reported. The cement industry uses the biomass as a substitute fuel for coal in the rotary kiln or in the cement calciner (Friege and Fendel, 2011; Pomberger et al., 2012). Cement calciners are pyroprocessing units positioned prior to the rotary kiln, just after the cyclone preheating system. Inside them, the temperature range from 800° to 950°C, and the calcination process occurs (Mikulčić et al., 2013b). Controlling the calcination and the combustion process inside cement calciners is of great importance, as these two reactions have a direct effect on the clinker quality and the amount of energy consumed (Koumboulis and Kouvakas, 2003). For this reason, several studies numerically investigated cement calciners. Giddings et al. (2000) numerically analysed a fully operating cement calciner. The work showed the usefulness of the CFD as a research tool and some important flow characteristics of the simulated calciner, which cannot be experimentally investigated. Huang et al. (2006a) performed a three-dimensional simulation of a new type swirl-spray calciner. The work showed that predicted results for limestone decomposition, coal burnout and the temperature at the exit of the calciner agreed well with measured results. Also Huang et al. (2006b) investigated the cement calciner's operating conditions to lower the NO_x emissions. The study showed that together air and fuel staging can lower the NO_x emissions. Mujumdar et al. (2007) studied the processes occurring in the preheater, the calciner, kiln and cooler, and developed a model for the simulation of these processes. The study showed that with respect to overall energy consumption, for the kiln process studied in this work, the optimum value of calcination in calciner is about 70%. Fidaros et al. (2007) presented a mathematical model and a parametric study of fluid flow and transport phenomena in a cement calciner. The work showed good prediction capabilities for temperature, velocity and distribution of limestone and coal particles at the calciner exit, where measurements exist. Zheng et al. (2012), using the large eddy simulation (LES) simulation approach and the kinetic theory of granular flow, investigated the mixing of particles and the stability of production for the simulated cement calciner. The study showed that operating parameters needed to be set up very precisely to have an efficient and a stable production. Mikulčić et al. (2013c) numerically investigated the influence of different amounts of fuel, mass flow of the tertiary air on the decomposition rate of limestone particles, burnout rate of coal particles and pollutant emissions of a newly designed cement calciner. The study showed that CFD is a useful tool for plant design and process improvements. All these studies show that there is still a need for further research of cement calciners, especially in the research of biomass combustion and co-firing in cement calciners.

The purpose of this paper is to present a CFD simulation of the co-combustion of biomass and coal in a cement calciner. Numerical models of pulverized coal and biomass combustion were developed and implemented into a commercial CFD code FIRE, which was then used for the analysis. By solving the governing set of conservation equations for mass, momentum and enthalpy, this code was used to simulate a turbulent flow field, interaction of particles with the gas phase, temperature field, and concentrations of the reactants and products. For biomass combustion, as well as for coal combustion, the effects of drying, the degradation during devolatilization, generation of gaseous species and char burnout were taken into account. Furthermore, three-dimensional geometry of a real industrial cement calciner was used for the CFD simulation of biomass and coal co-firing process.

Numerical model

The motion and transport of the solid particles are tracked through the flow field using the Lagrangian formulation, while the gas phase is described by solving conservation equations using the Eulerian formulation. Solid particles are discretized into finite numbers of particle groups, known as parcels, which are supposed to have same size and the same physical properties. The parcels are tracked as they move through the calculated flow field by using a set of equations derived from mass, momentum and enthalpy balances. The coupling between the parcels and the gaseous phase is taken into account by introducing appropriate source terms for mass, momentum and enthalpy exchange. The heterogeneous reactions of the mathematical model used for the calcination process, coal and biomass combustion calculation are treated in the Lagrangian spray module, where thermo-chemical reactions occur, involving particle components and gas phase species. The homogeneous reactions used for the coal and biomass combustion calculation are treated in the gas phase using the Eulerian formulation.

The developed models, together with thermo-physical properties of the limestone, the lime and the components of the biomass and coal particles, as well as a particle radiation model, were integrated into the commercial CFD code via user-functions written in the FORTRAN programming language, in order to simulate the named thermo-chemical reactions properly (Baburić et al., 2004).

Continuous phase

The equations of continuum mechanics are based on the conservation laws for mass, momentum and energy. The general form

Downloaded from wmr.sagepub.com by guest on July 10, 2014

of the time averaged conservation equation for any dependent variable φ, of the continuous phase in the differential form is:

$$\frac{\partial}{\partial t}(\rho\varphi)+\frac{\partial}{\partial x_j}(\rho\varphi u_j)=\frac{\partial}{\partial x_j}(\Gamma_\varphi\frac{\partial\varphi}{\partial x_j})+S_\varphi, \quad (1)$$

where ρ is the density, u_j Cartesian velocity, Γ_φ diffusion coefficient and S_φ is the source term of the dependent variable φ. The source term S_φ is used for the coupling of the Eulerian and the Lagrangian phase.

Calcination process

In general, the following equation presents the calcination process:

$$CaCO_3(s)\xrightarrow{+\ 178\ kJ\ mol^{-1}}CaO(s)+CO_2(g). \quad (2)$$

To describe the calcination process, a numerical model previously developed and validated was used (Mikulčić et al., 2012). The developed model takes into account the effects of decomposition pressure, temperature, diffusion and pore efficiency. It is detailed enough to contain the relevant physical and chemical processes, yet simple enough for detailed CFD simulations.

Pulverized coal and biomass combustion

The combustion of biomass can be considered, by analogy to coal combustion, as a four-step process: drying, devolatilization, char combustion and volatile combustion. For coal combustion models, the process of drying is incorporated in the devolatilization models. However, for biomass combustion, the water content is of significant importance and dominates the combustion process.

The evaporation of water vapour is related to the difference in water vapour concentration at the particle surface and in the gas:

$$N_w=k_w(C_p-C_g), \quad (3)$$

where N_w is the molar flux of water vapour, k_w is the mass transfer coefficient, C_p is the water vapour concentration at the particle surface and C_g is the water vapour concentration in the gas.

The water vapour concentration at the particle surface is evaluated by assuming that the partial pressure of water vapour at the particle surface is equal to the saturated water vapour pressure p_{sat}, at the particle temperature T_p:

$$C_p=\frac{p_{sat}}{RT_p}, \quad (4)$$

where R is the universal gas constant.

The concentration of vapour in the gas is known from solution of the following equation:

$$C_g=X_{H2O}\frac{p}{RT}, \quad (5)$$

where X_{H20} is the total local water mole fraction, which includes the air moisture, evaporated moisture, and combustion products of coal and biomass, p is the local absolute pressure, and T is the local temperature in the gas. The mass transfer coefficient is calculated from the Sherwood number correlation:

$$Sh_{AB}=\frac{k_w d_p}{D_w}=2.0+0.6\,\mathrm{Re}_p^{1/2}Sc^{1/3}, \quad (6)$$

where d_p is the particle diameter, Re_p is the particle Reynolds number and Sc is the Schmidt number. The Schmidt number is calculated according the following equation:

$$Sc=\frac{\mu}{\rho D_w}, \quad (7)$$

where μ is the dynamic viscosity, ρ is the density and D_w is the diffusion coefficient of water vapour in the gas.

The water vapour flux becomes a source of water vapour in the gas phase species transport equation, and the mass flux of water vapour multiplied by the latent heat becomes a source in the energy equation.

$$m_p c_p\frac{dT_p}{dt}=\alpha A_p(T_g-T_p)+\varepsilon_p\sigma A_p(T_g^4-T_p^4)+\frac{dm_p}{dt}h_{latent} \quad (8)$$

In Eq. 8, m_p is the particle mass, c_p is the particle heat capacity, T_p is the particle temperature, T_g is the surrounding gas temperature, A_p is the particle surface, α is the convective heat transfer coefficient, ε_p is the particle emissivity, σ is the Stefan–Boltzmann constant and h_{latent} is the latent heat.

When the particle reaches the boiling temperature, i.e. 100°C, the boiling of particulate water starts. During the entire boiling process, the particle temperature remains the same, until the entire capillary bounded water is vaporized (Ma et al., 2007).

For devolatilization, a single rate expression is used meaning that the devolatilization rate $dc_{biomass}/dt$ is in a first-order dependency on the amount of biomass remaining in the particle:

$$\frac{dc_{biomass}}{dt}=-k_1 y_{biomass} \quad (9)$$

Here $y_{biomass}$ is the mass fraction of biomass remaining in the particle and k_1 is the kinetic rate defined by an Arrhenius-type expression, including a pre-exponential factor ($k_{0,1}$) and an activation energy (E_1):

$$k_1=k_{0,1}\exp\left(-E_1/RT_p\right) \quad (10)$$

The values of the kinetic constants ($k_{0,1}$, the pre-exponential factor; E_1, the activation energy) for different biomass devolatilization are obtained from the literature (Ma et al., 2007).

Parallel to the devolatilization, char is oxidized to form CO and CO_2 taking into account a mechanism factor depending on char particle size and temperature:

Downloaded from wmr.sagepub.com by guest on July 10, 2014

Table 1. Boundary conditions.

	T (°C)	Reference case (100% coal combustion)	Case 1 (biomass 10% energy substitution)	Case 2 (biomass 20% energy substitution)	Case 3 (biomass 30% energy substitution)
		Mass flow rate (kg h^{-1})			
Limestone 1+2	720	147 900			
Tertiary air 1	950	49 600			
Tertiary air 2	950	49 600			
Primary air	80	16 200			
Secondary air	950	33 065			
Coal	60	14 811	13 330	11 848	10 368
Biomass	60	–	3944	7888	11 833
Hot gas from rotary kiln	1100	110 600			
Outlet (Static Pressure)		10^5 Pa	10^5 Pa	10^5 Pa	10^5 Pa

$$C+\frac{1}{f_m}O_2 \xrightarrow{\substack{-395\ kJ\ mol^{-1}\\ -110\ kJ\ mol^{-1}}} \left(2-\frac{2}{f_m}\right)CO+\left(\frac{2}{f_m}-1\right)CO_2 \quad (11)$$

In Eq. 11, f_m represents the mechanism factor, which ranges between 1 and 2, causing predominant generation of CO for higher temperatures of approximately 900 K, and predominant production of CO_2 for temperatures lower than 900 K (Görner, 1991).

Char combustion (Eq. 11) is modelled according to the kinetics/diffusion limited reaction model of Baum and Street (1971). The model assumes that the reaction rate of char combustion is limited by either the kinetics of the heterogeneous reaction k_2^{ch} or the oxygen's diffusion into the particle's mass expressed by the value of k_2^{ph}:

$$\frac{dc_c}{dt} = -k_2 A_p p_{ox} y_c \quad (12)$$

$$k_2 = \frac{k_2^{ch} \cdot k_2^{ph}}{k_2^{ch} + k_2^{ph}} \quad (13)$$

$$k_2^{ch} = k_{0,2}^{ch} \cdot \exp\left(-E_2^{ch} / RT\right) \quad (14)$$

$$k_2^{ph} = \frac{24 \cdot f_m \cdot D_0}{R \cdot d_p \cdot T_0^{1.75}} T^{0.75} \cdot 10^5 \quad (15)$$

In Eq. 12 the char reaction rate dc_c/dt in terms of rate of change of mass fraction is given. Here y_c is the mass fraction of char remaining in the particle, A_p is the specific particle surface, p_{ox} is the oxygen partial pressure and k_2 is the overall kinetic rate of char combustion. In Eq. 14, the kinetics of the heterogeneous reaction k_2^{ch} is defined as an Arrhenius-type expression with a pre-exponential factor $k_{0,1}^{ch}$ and activation energy E_2^{ch}. In Eq. 15, D_0 is the oxygen diffusion coefficient, d_p is the particle diameter and T_0 is the reference temperature. The values of the kinetic constants for the char combustion model are obtained from the literature (Görner, 1991).

For the combustion of the volatiles released during the devolatilization process, a detailed chemistry approach is used for each of the homogeneous reaction. The source terms accounting for the gas phase reactions in the species transport equations and in the gas phase energy equation are calculated with reaction rates depending on species concentrations and temperature, e.g. reaction rates are defined by an Arrhenius law. The modelled homogeneous reactions include tar and CO oxidation, NO_x formation and the combustion of methane (Mikulčić et al., 2013c).

Computational details of the simulated cement calciner

To demonstrate the biomass combustion application, a three-dimensional geometry of an industrial cement calciner was used for a numerical simulation of biomass and coal co-firing. A detailed description of the geometry and the boundary conditions of the modelled calciner can be found in our previous study (Mikulčić et al., 2013c).

The grid-size dependency for calcination calculation was analysed in our previous study (Mikulčić et al., 2012), and based on these results, in the simulation of a cement calciner, 47 000 cells were employed to discretize the computational domain. The differencing scheme used for momentum, continuity and enthalpy balances was MINMOD Relaxed (FIRE Manuals, 2011) and for turbulence and scalar transport equations an Upwind scheme was applied. Turbulence was modelled by the standard $k-\varepsilon$ model. The P-1 radiation model was used to model the radiative heat transfer and the effects of the particle.

Since it is well known that the use of alternative fuels in existing pulverized burners alters the flame shape and the temperature profile inside the furnace (Beckmann et al., 2012), three different co-firing cases were simulated. The boundary conditions used for these three co-firing cases are given in Table 1. Furthermore, for consistency and better understanding of the amount of fuel that was substituted, in Table 1 the boundary conditions used for the reference coal combustion case are summarized. The values for the reference coal combustion case were the input data that were provided to the authors (Mikulčić et al., 2013c). The proximate and ultimate analyses of the used coal and biomass are tabulated in Table 2.

Downloaded from wmr.sagepub.com by guest on July 10, 2014

Result and discussion

Figure 1 shows the streamlines of the flow inside the calciner for the three calculated co-firing cases. It can be observed that in each case, in the left calciner part, the flow is highly swirled. The reason for this highly swirled flow is the large mass flow of the tertiary air that enters at the top of the calciner. The highly swirled flow enhances the mixing of particles, and the majority of reactions occur in this part of the calciner. What can also be observed is a small difference in the flow of the three co-firing cases. From left to right it can be observed that the streamlines are due to the larger fuel mass load in Case 1 and Case 2 moved from the connecting cylinder top wall to its centre.

Table 2. Proximate and ultimate analysis of the used coal and biomass.

	Coal	Biomass
Proximate (%wt raw)		
Moisture	0.5	33.00
Volatile matter	29.68	31.97
Fixed carbon	54.82	20.03
Ash	15.0	15.0
Ultimate (%wt daf)		
C	82.94	48.40
H	2.62	7.65
O	9.33	39.16
N	2.31	2.79
S	1.00	1.00
Lower heating value (MJ kg^{-1})	25.34	9.51

daf, dry ash free.

In Figure 2, the temperature field inside the calciner for the three calculated co-firing cases is shown. It can be seen that in all three cases in the left calciner part, temperatures in the near wall region are lower than in the centre. This is due to the calcination process, which is a strong endothermic reaction. Furthermore, when comparing the co-firing cases with the case where only the coal was combusted (Mikulčić et al., 2013c), it can be observed that in the co-firing cases in the near burner region the temperatures are roughly 100 K lower.

Figure 3 shows the CO_2 mole fraction inside the calciner for the three calculated co-firing cases. It is known that the majority of CO_2 emissions from cement manufacturing come from the calcination process. Since in modern cement plants calcination occurs in cement calciners, very high concentrations of CO_2 can be found in these units. In all three calculated cases, the highest concentration of CO_2 is in the connecting cylinder, where most of the calcination process takes place.

Figure 4 shows the limestone mass fraction in particles and their distribution inside the calciner for the three calculated co-firing cases. As can be observed, limestone mass fraction decreases from the calciner's inlet towards the outlet, and in all three cases the position of limestone particles is similar. The 'empty' calciner regions in this figure indicate the regions where conversion of limestone to lime has largely already been completed.

Figure 5 shows the lime mass fraction in particles and their distribution inside the calciner for the three calculated co-firing cases. As can be observed due to the available heat provided by the fuel combustion, the limestone decomposes and

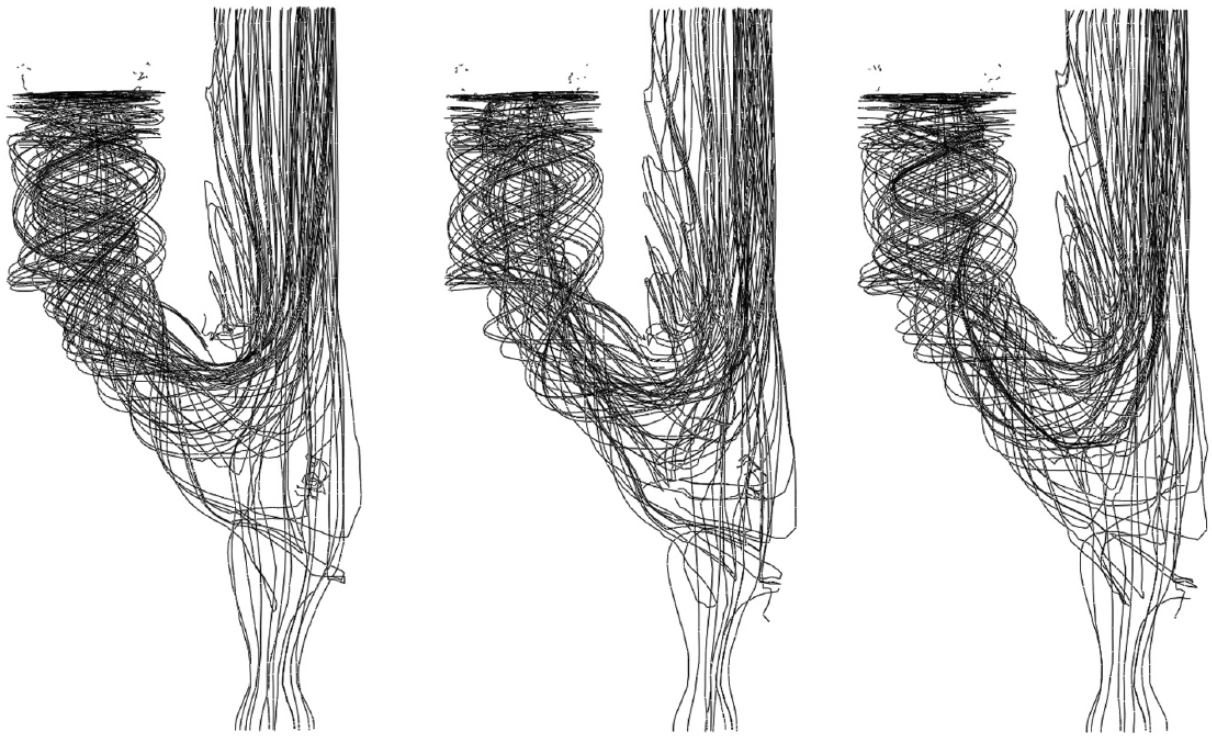

Figure 1. Flow characteristics inside the calciner: Case 1 (left); Case 2 (middle); Case 3 (right).

Downloaded from wmr.sagepub.com by guest on July 10, 2014

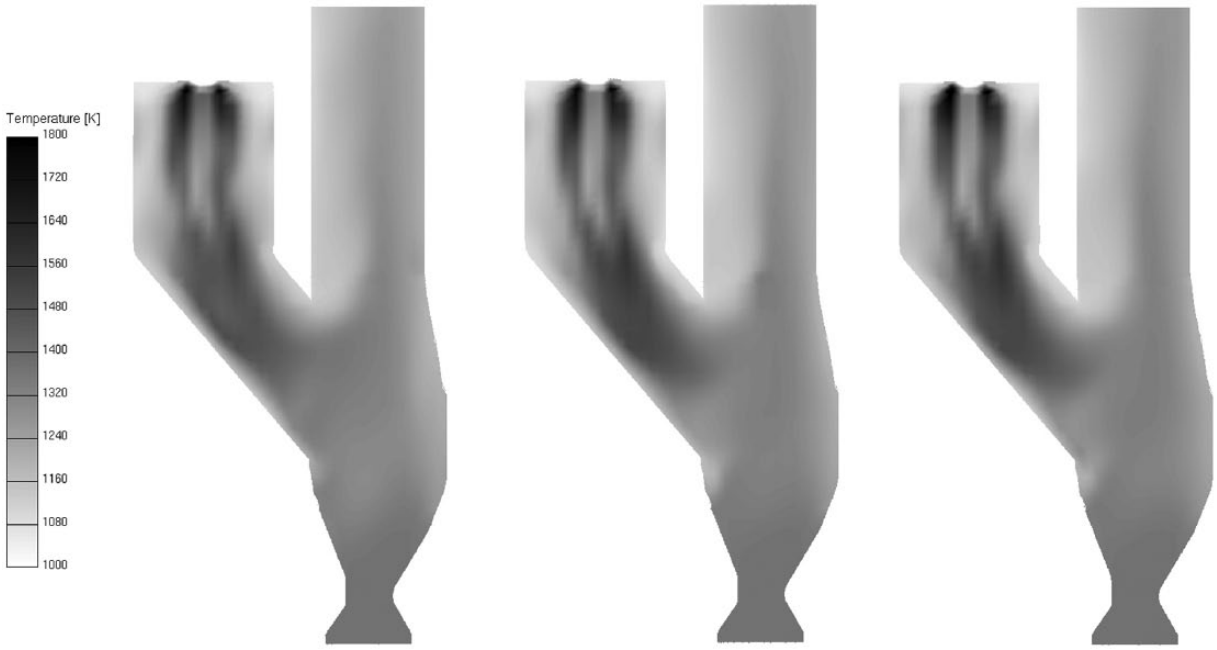

Figure 2. Temperature field inside the calciner: Case 1 (left); Case 2 (middle); Case 3 (right).

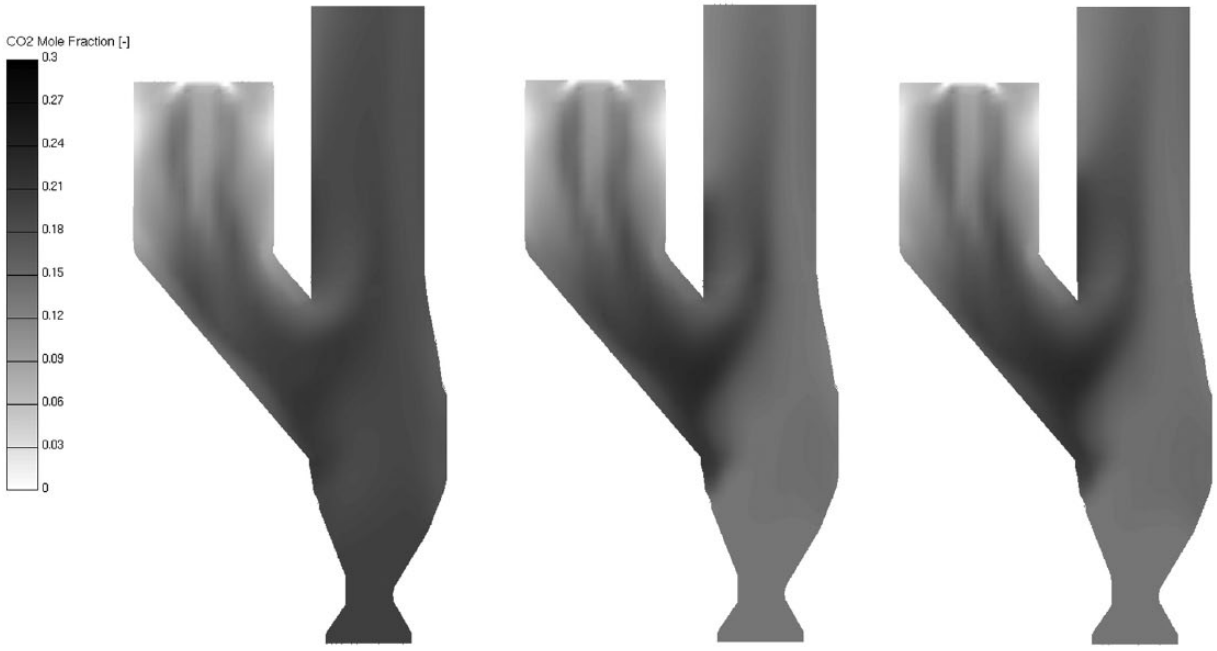

Figure 3. CO_2 mole fraction inside the calciner: Case 1 (left); Case 2 (middle); Case 3 (right).

the lime mass fraction increases from the calciner's inlet towards the outlet.

Figure 6 shows the char mass fraction in particles and their distribution inside the calciner for the three calculated co-firing cases. It can be seen that in all three cases the char particles are located in the middle of the left calciner part, where most of it oxidizes, and afterwards the high-velocity upward stream in the right part of the calciner blows them towards the outlet. Here it should be noted that in all three co-firing cases a small amount of unburned char particles exit the calciner, which was not observed when just coal was combusted (Mikulčić et al., 2013c). The reason for this is the prolonged combustion time of the biomass particles. The biomass particles, which contain significantly more humidity than coal particle, first have to dry, then undergo devolitilization and after that the formed char particle needs to oxidize. For a plant operator, this information is essential, since it is not desirable to have some burnout char particles in the preheating system. The reason is that char particles can still oxidize in cement cyclones, causing destabilization of the preheating process and formation of undesirable pollutants.

Downloaded from wmr.sagepub.com by guest on July 10, 2014

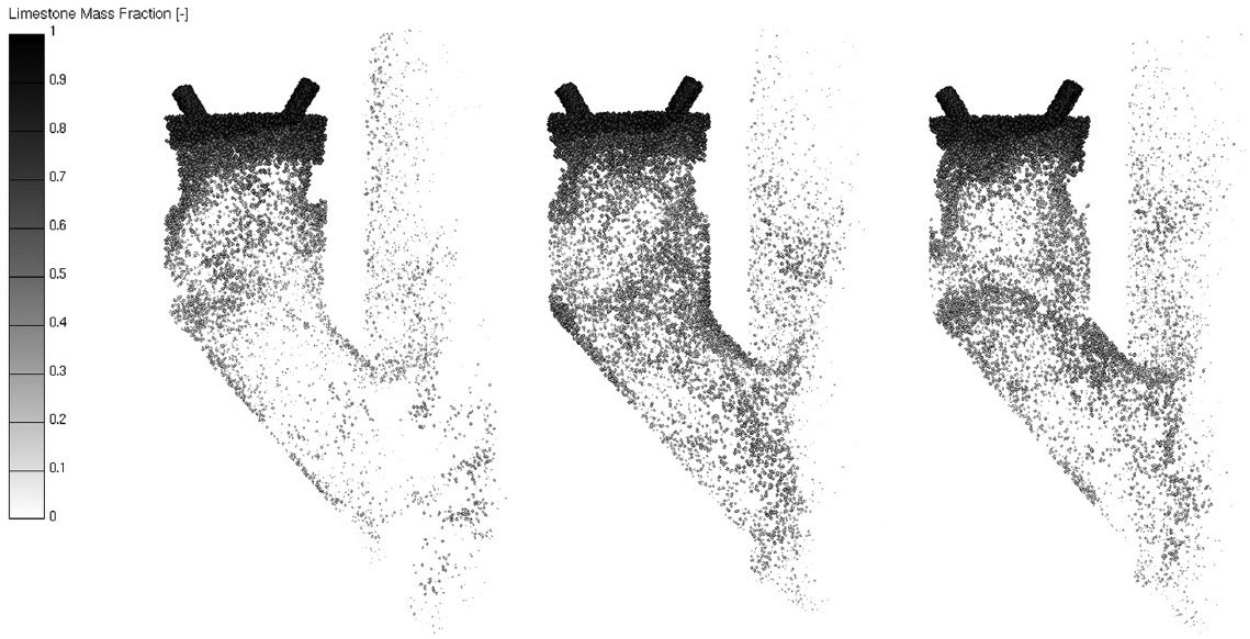

Figure 4. Limestone ($CaCO_3$) mass fraction in particles: Case 1 (left); Case 2 (middle); Case 3 (right).

Figure 5. Lime (CaO) mass fraction in particles: Case 1 (left); Case 2 (middle); Case 3 (right).

Figure 7 shows a comparison of the char burnout and limestone decomposition ratios on the calciner outlet for the three calculated co-firing cases. It can be seen that all three cases have similar burnout and decomposition ratios; however, when comparing these results with burnout and decomposition ratios of a calciner operating fully on coal, the difference can be seen. The co-firing cases have lower burnout and decomposition ratios. This can be explained by the prolonged combustion time of the biomass particles.

To ensure adequate conditions for a complete calcination reaction inside cement calciners, extensive understanding of the biomass and coal co-firing process is needed. Precisely the results gained by this study show that the developed models, coupled with a commercial CFD code, form a promising tool for improvement of the understanding of the co-firing process.

Conclusion

A numerical analysis of the co-firing of pulverized biomass and coal inside a cement calciner is presented. Numerical models of pulverized coal and biomass combustion were developed and

Downloaded from wmr.sagepub.com by guest on July 10, 2014

Figure 6. Char mass fraction in particles: Case 1 (left); Case 2 (middle); Case 3 (right).

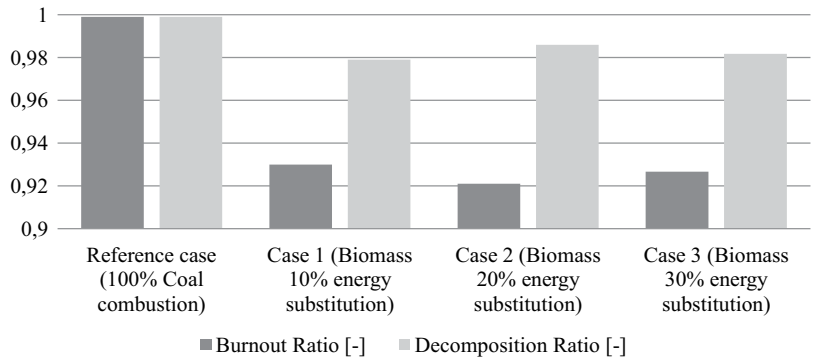

Figure 7. Comparison of burnout and decomposition ratios.

implemented into a commercial CFD code FIRE, which was then used for the analysis. The Eulerian–Lagrangian approach was used for coupling of the gaseous and particle phase. For the pulverized coal and biomass combustion, the effects of drying, devolatilization, char oxidation and volatile combustion are taken into account. For the calcination process, the effects of decomposition pressure, temperature, diffusion and pore efficiency are taken into account. Three-dimensional geometry of a real industrial cement calciner was used for the analysis. Three different co-firing cases were analysed. The results show that when combusting biomass in existing pulverized-fuel burners, special attention needs to be given to the complete oxidation of the char particles, in order to avoid undesirable instabilities in the preheating system. Furthermore, from the results shown it can be concluded that numerical modelling of the co-firing of biomass and coal can assist in improving the understanding of the co-firing process, in the investigation and better understanding of particle kinetics, in the optimization of cement calciner's operating conditions and finally in reducing pollutant formation in combustion units.

Acknowledgements

The authors wish to thank Dr P Priesching and Dr R Tatschl, from the CFD Development group at AVL-AST, Graz, Austria, for their continuous support and useful discussions during the development of numerical models used in this study.

Declaration of conflicting interests

The authors declare that there is no conflict of interest.

Funding

The research was conducted with the financial support from AVL List GmbH, Graz, Austria.

Downloaded from wmr.sagepub.com by guest on July 10, 2014

References

Baburić M, Raulot A and Duić N (2004) Implementation of discrete transfer radiation method into SWIFT computational fluid dynamics code. *Thermal Science* 8: 293–301.

Baum MM and Street PJ (1971) Predicting the combustion behaviour of coal particles. *Combustion Science and Technology* 3: 231–243.

Beckmann M, Pohl M, Bernhardt D and Gebauer K (2012) Criteria for solid recovered fuels as a substitute for fossil fuels – a review. *Waste Management & Research* 30: 354–369.

Ćosić B, Stanić Z and Duić N (2011) Geographic distribution of economic potential of agricultural and forest biomass residual for energy use: case study Croatia. *Energy* 36: 2017–2028.

Fidaros DK, Baxevanou CA, Dritselis CD and Vlachos NS (2007) Numerical modelling of flow and transport processes in a calciner for cement production. *Powder Technology* 171: 81–95.

FIRE v2011 Manuals (2011) Graz, Austria.

Fodor Z and Klemeš JJ (2012) Waste as alternative fuel – minimising emissions and effluents by advanced design. *Process Safety and Environmental Protection* 90: 263–284.

Friege H and Fendel A (2011) Competition of different methods for recovering energy from waste. *Waste Management & Research* 29: 30–38.

Giddings D, Eastwick CN, Pickering SJ and Simmons K (2000) Computational fluid dynamics applied to a cement precalciner. *Proceedings of the Institution of Mechanical Engineers, Part A: Journal of Power and Energy* 214: 269–280.

Görner K (1991) *Technische Verbrennungssysteme: Grundlagen, Modellbilung, Simulation* (*Technical combustion systems: fundamentals, modelling, simulation*), pp. 180–194. Berlin: Springer.

Huang L, Lu J, Xia F, Li W and Ren H (2006a) 3-D mathematical modeling of an in-line swirl-spray precalciner. *Chemical Engineering and Processing: Process Intensification* 45: 204–213.

Huang L, Lu J, Hu Z and Wang S (2006b) Numerical simulation and optimization of NO emissions in a precalciner. *Energy & Fuels* 20: 164–171.

Lu H, Robert W, Peirce G, Ripa B and Baxter LL (2008) Comprehensive study of biomass particle combustion. *Energy & Fuels* 22: 2826–2839.

Koumboulis FN and Kouvakas ND (2003) Model predictive temperature control towards improving cement precalcination. *Proceedings of the Institution of Mechanical Engineers, Part I: Journal of Systems and Control Engineering* 217: 147–153.

Klemeš JJ, Varbanov PS, Pierucci S and Huisingh D (2010) Minimising emissions and energy wastage by improved industrial processes and integration of renewable energy. *Journal of Cleaner Production* 18: 843–847.

Ma L, Jones JM, Pourkashanian M and Williams A (2007) Modelling the combustion of pulverized biomass in an industrial combustion test furnace. *Fuel* 86: 1959–1965.

Mikulčić H, von Berg E, Vujanović M, Priesching P, Perković L, Tatschl R and Duić N (2012) Numerical modelling of calcination reaction mechanism for cement production. *Chemical Engineering Science* 69: 607–615.

Mikulčić H, Vujanović M and Duić N (2013a) Reducing the CO_2 emissions in Croatian cement industry. *Applied Energy* 101: 41–48.

Mikulčić H, Vujanović M, Markovska N, Filkoski RV, Ban M and Duić N (2013b) CO_2 emission reduction in the cement industry. *Chemical Engineering Transactions* 35: 703–708.

Mikulčić H, von Berg E, Vujanović M, Priesching P, Tatschl R and Duić N (2013c) Numerical analysis of cement calciner fuel efficiency and pollutant emissions. *Clean Technologies and Environmental Policy* 15: 489–499.

Momeni M, Yin C, Kær SK and Hvid SL (2013) Comprehensive study of ignition and combustion of single wooden particles. *Energy & Fuels* 27: 1061–1072.

Mujumdar KS, Ganesh KV, Kulkarni SB and Ranade VV (2007) Rotary Cement Kiln Simulator (RoCKS): integrated modeling of pre-heater, calciner, kiln and clinker cooler. *Chemical Engineering Science* 62: 2590–2607.

Pomberger R, Klampfl-Pernold H and Abl C (2012) Current issues on the production and utilization of medium-calorific solid recovered fuel: a case study on SRF for the HOTDISC technology. *Waste Management & Research* 30: 413–420.

Ragossnig AM, Wartha C and Pomberger A (2009) Climate impact analysis of waste treatment scenarios – thermal treatment of commercial and pretreated waste versus landfilling in Austria. *Waste Management & Research* 27: 914–921.

Schneider DR and Ragossnig AM (2013) Biofuels from waste. *Waste Management & Research* 31: 339–340.

Sommer M and Ragossnig A (2011) Energy from waste in Europe: an analysis and comparison of the EU 27. *Waste Management & Research* 29: 69–77.

Thomanetz E (2012) Solid recovered fuels in the cement industry with special respect to hazardous waste. *Waste Management & Research* 30: 404–412.

Vad Mathiesen B, Lund H and Connolly D (2012) Limiting biomass consumption for heating in 100% renewable energy systems. *Energy* 48: 160–168.

Williams A, Jones JM, Ma L and Pourkashanian M (2012) Pollutants from the combustion of solid biomass fuels. *Progress in Energy and Combustion Science* 38: 113–137.

Yang YB, Sharifi VN, Swithenbank J, Ma L, Darvell LI, Jones JM, Pourkashanian M and Williams A (2008) Combustion of a single particle of biomass. *Energy & Fuels* 22: 306–316.

Zheng Jianxiang, Yan Tingzhi and Yang Jing (2012) Numerical simulation of gas and solid flow behaviour in the pre-calciner with large eddy simulation approach. *Energy Procedia* 17: 1535–1541.

Downloaded from wmr.sagepub.com by guest on July 10, 2014